



Experimental and theoretical investigation of the particle size effect on XRF intensity for some metals nanopowders in liquid media

A.Kadhim¹, Ahmed A. Al-Amiery², Razi J.Alazawi¹, Raid S.Jawad³

¹Laser and optoelectronic Engineering Department, University of Technology, Baghdad, Iraq

²Environment research center, University of Technology, Baghdad 10066, Iraq

³Energy and renewable energies technology center

Email: abdulhadikadhim5@gmail.com, dr.ahmed1975@gmail.com, dr99990@yahoo.in

Abstract

Different particle sizes from Iron, Cobalt, and Nickel nanopowders were prepared and subjected to He-Ne laser system to determine the particle size. Samples were prepared by blending 1wt% of each metal powders at a time and 99wt% of food oil. Microscopic examination was carried out for all samples to reveal the particle size distribution. X-ray spectrometer was used to characterize and analyze the samples. X-ray intensities were determined experimentally and theoretically for prepared samples. Consensus acceptable between theoretical and experimental results was found.

© 2017 ijrei.com. All rights reserved

Keywords: Ray intensity, particle size, metal powder, food oil

1. Introduction

X-Ray Fluorescence (XRF) is capable of measuring fine particles as well as plate metal sample, however, it is limited by the depth to which the X-rays are capable of exciting the sample. This leads to a particle size effect [1]. It is difficult to obtain successful X-ray control of materials without some understanding of the effect of the two most important variables influencing X-ray intensities in suspended samples namely particle size and homogeneity [2, 3]. In addition to its use in determination of organometallics and dissolved metals, XRF has been applied to suspended metal particulate in food oil [4]

1.1 Theoretical part

When X-ray passes through the object being tested, the signal is attenuated by scattering and absorption according to Beers law.

$$I = I_0 e^{-\mu x} \quad (1)$$

Where I_0 : the initial intensity.

I : the final intensity.

μ : the attenuation coefficient (cm^{-1}).

x : the length of X-ray path (cm).

But the actual volume of sample which can contribute to the measured fluorescent radiation is independent upon the effective penetration depth of the measured wave length [5, 6]. This in turn supports need for completely homogenous specimen. Since if for instance compositional variation in depth is present if we consider a powder sample containing the element of interest in spherical particles of a uniform diameter D , then at any depth of χ from the surface there are likely to be N particles, where N is proportional to the concentration of the element. If the original particle diameter is reduced to $(D/2)$, then at the same depth χ there will be $(8N)$ particles. If the particles are cubic in shape then the particle size reduction again results in an eight fold increase in number and can be described as a lateral displacement of the lower half of the cubic. The exciting radiation is again absorbed by the matrix until it reaches the surface and is measured. Assuming the average depth of particles is the same for the different particle size [7, 8], then the total matrix absorption is virtually independent of particle size. It is evident that for cubic particles reducing the dimension of a side by two is equivalent to exposing twice the original area of the material being measured at a half of the original thickness. In the spherical particle the same is true since the surface area of a sphere is proportional to the diameter squared [9, 10]. It is a

well-known fact that the intensity of a characteristic line emitted by a thin layer of material increases the thickness is increased up to a point which we will define as infinite thickness, value any increase in thickness will result in no observable gain in characteristic signal from the sample [11, 12]. The relationship between the fluorescent intensity from the same sample infinite thickness of which can be shown to be as follows [13, 14].

$$(I_x/I_\infty) = 1 - \text{EXP}(-a\rho\chi_c) \tag{2}$$

Where I_x and I_∞ are the intensities of fluorescent radiation per square centimeter leaving samples of thickness χ and ∞ respectively.

a : the absorption parameter .

ρ : the density of sample .

χ_c : the critical thickness of sample .

$$a = \mu_i \csc\theta_i + \mu_e \csc\theta_e \tag{3}$$

Where μ_i and μ_e are the absorption coefficients for incident and emergent X-ray respectively. θ_i and θ_e are the incident and emergent angles respectively . The effect of inhomogeneity of particle size within samples of one compound was studied, the smallest size showed to yield highest intensities [15]

1.2 Theoretical calculations

In order to determine infinite thickness from the equation (2) we arbitrarily choose a value of 0.99 for the ratio of (I_x/I_∞) . We can define particle size in terms of the infinite thickness value, and by using the equation (3) the absorption parameter (a) can be calculated from the data as shown in Table 1. The values of μ_i and μ_e were determined by using software program [16-19], θ_e values from ref [16], and $\theta_i = 52.5$ for XFR system which was used in this work.

Table 1 the values of absorption coefficients and diffracted angles of element used in this work .

Element	μ_i (cm ² /g) at operated energy (0.41°A)	μ_e (cm ² /g) at K_α line	θ_e	a (cm ² /g)	χ_c (μm)
Iron	7.09	71.04	57.46	93.202	62.5
Cobalt	7.86	78.47	52.74	108.497	47.69
Nickel	8.65	91.26	48.6	132.313	39.11

Now the critical area for Iron , Cobalt , and Nickel can be calculated by using the critical thickness (table-1) and considered the shape of particles is spherical , and these values equal to 1.23×10^{-4} cm² for Fe , 7.14×10^{-5} cm² for Co , and 4.8×10^{-5} cm² for Ni , and the another step represents calculation of the real area by using the measured average particle size as shown in tables (2-4) for Fe , Co , and Ni respectively.

Table 2 Particle size, area, and number of times of real area increased over critical area of Iron samples

Average particle size (cm)	Area (cm ²)	No. of times of real area increased over critical area
0.022	0.00152	12.39
0.024	0.00181	14.74
0.03	0.00282	23.04
0.032	0.00321	26.21

Table 3 Particle size , area , and number of times of real area increased over critical area of Cobalt samples

Average particle size (cm)	Area (cm ²)	No. of times of real area increased over critical area
0.0055	0.000094	1.33
0.006	0.000113	1.58
0.0065	0.000132	1.86
0.0075	0.000176	2.473

Table .4 Particle size , area , and number of times of real area increased over critical area of Nickel samples

Average particle size (cm)	Area (cm ²)	No. of times of real area increased over critical area
0.0075	0.000176	3.68
0.0085	0.000227	4.72
0.0105	0.000346	7.21
0.0115	0.000415	8.65

"No. of times of real area increased over critical area means the ratio of the real area and critical area"

Now we can calculate the theoretical relative intensity (I/I_0) for all suspended samples as shown in table 5

Table .5 Theoretical relative intensity for Fe , Co , and Ni suspended in Iraqi oil .

Samples	Average particle size (cm)	Theoretical relative intensity
Fe	0.022	0.729
	0.024	0.698
	0.03	0.617
	0.032	0.593
Co	0.0055	0.981
	0.006	0.974
	0.0065	0.965
	0.0075	0.946
Ni	0.0075	0.909
	0.0085	0.88
	0.0105	0.82
	0.0115	0.791

2. Experimental part

2.1 Sample preparation

The average particle size measurements for Fe, Co, and Ni powders were conducted by using different sieving of range (20-300 μm) and subjected to He-Ne laser system (made in USA) with wave length of 632 nm and power of 1mwatt to determine the experimental average particle size for Fe, Co and Ni powders with more accurate. Fe, Co and Ni powders of different particle sizes were blended with engines oil of SAE-40HD whose flash point is 236 $^{\circ}\text{C}$, viscosity at 100 $^{\circ}\text{C}$ is 15 cSt, and pour point is at -9 $^{\circ}\text{C}$ [17]. Mixture containing 1wt% Fe, Co or Ni powders of different particle sizes and 99wt% of oil were made by blending manually with care and by using an ultrasonic generator of Japan product. Microscopic examination was conducted for all suspended samples to reveal the particle size distribution in oil matrix, Microscopic examination carried out by used optical microscope with digital camera, and the mixture was placed in special container on microscope stage.

2.2 XRF intensity measurements

The XRF system type Simiens of Germany product was operated at fixed operation conditions of 30KV and 17mA. All samples were placed in liquid samples container and then fitted to X-ray fluorescence system to conduct XRF intensities of Fe K_{α} , Co K_{α} , and Ni K_{α} lines in (count/10s) and averaged to (count/s). to evaluate the effect of particle size on XRF intensity.

3. Results and discussion

Fig. 1 to 3 represents the microscopic examination of 1 wt% of Fe, Co, and Ni of different particle sizes suspended in oil. Fig. 4 to 6 represents the XRF theoretical relative intensity and real intensity (which was calculated as the peak intensity of suspended samples to the peak intensity for the pure sample) for Fe, Co and Ni powders suspended in oil as a function of particle sizes. These figures exhibited the results of XRF measurements which were determined theoretically and experimentally for different particle sizes. Particles of the smallest size were shown to yield the highest intensities while particles of the largest sizes were shown to yield lowest intensities for all specimens. The behavior of the intensity curve due to the increase in intensity was attributed to a decrease in voids of the specimen surface with the reduction in particle size. This leads to the larger excitation area. Some differences between the theoretical intensity and the real intensity are due to statistical errors in XRF measurements and to electrical noise and they may also be due to the sample preparation method. These results agreement with some references [2, 10]. This research can be applied in the field of NDT inspections of different engines or transformer by determined the type of derbies metals in oils, and in the field of oil analysis.

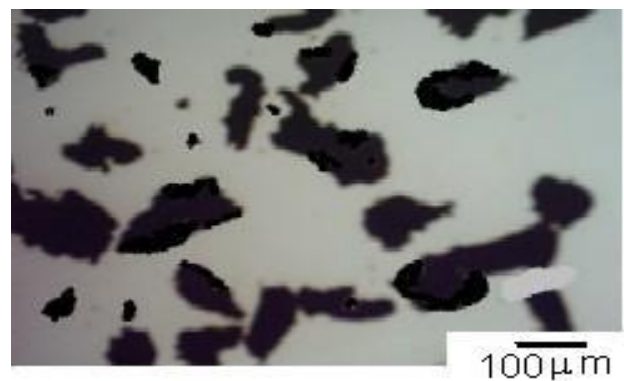
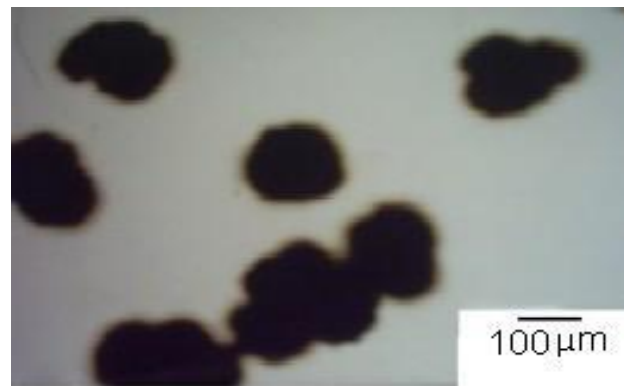
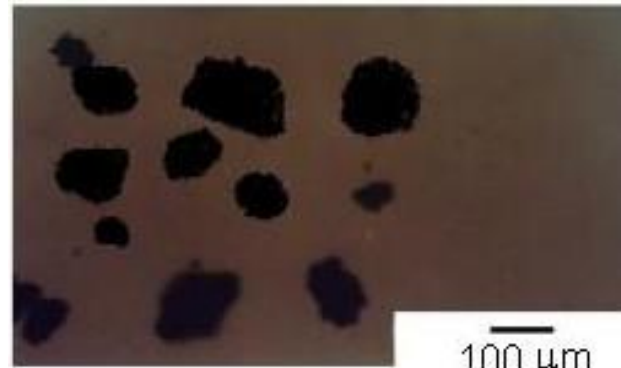
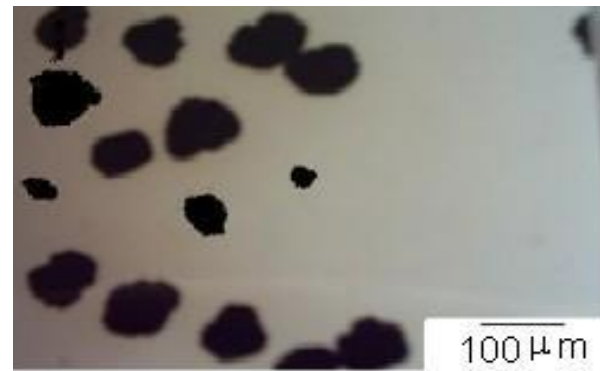


Figure 1: Microscopic photograph of Iron nanopowder suspended in oil at different particle sizes x 100

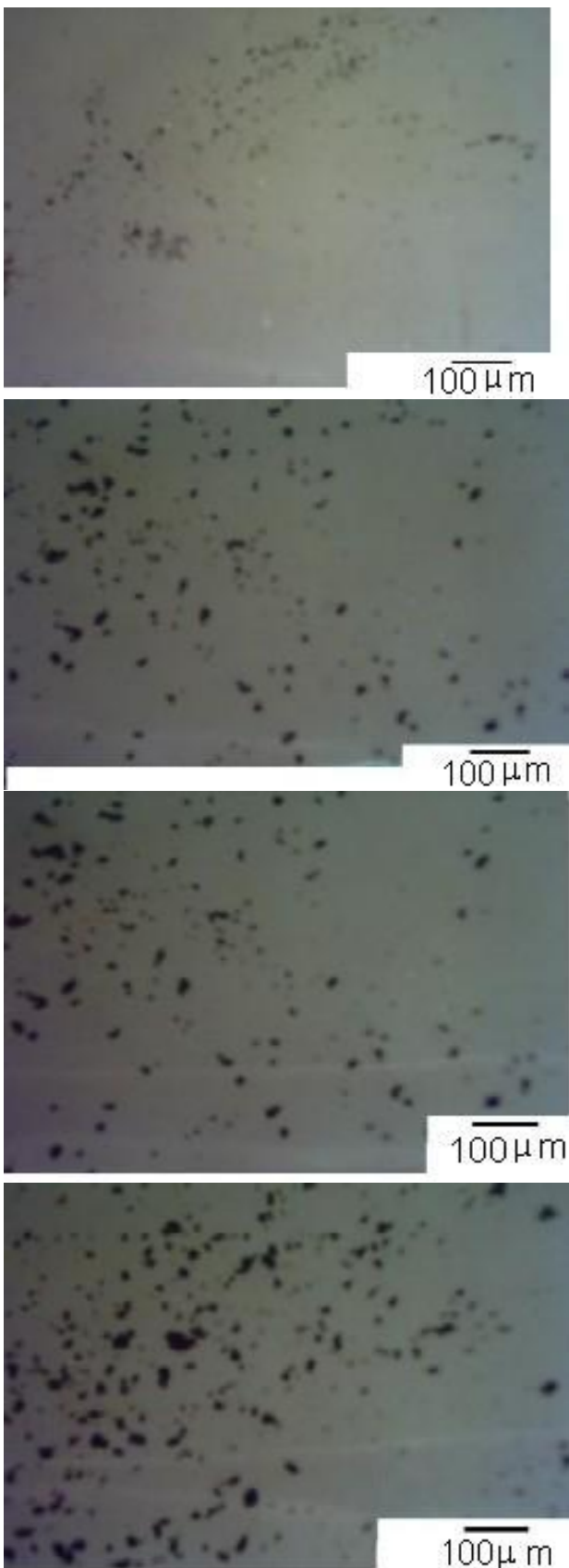


Figure 2: Microscopic photograph of Cobalt nanoparticles suspended in oil at different particle sizes .x100

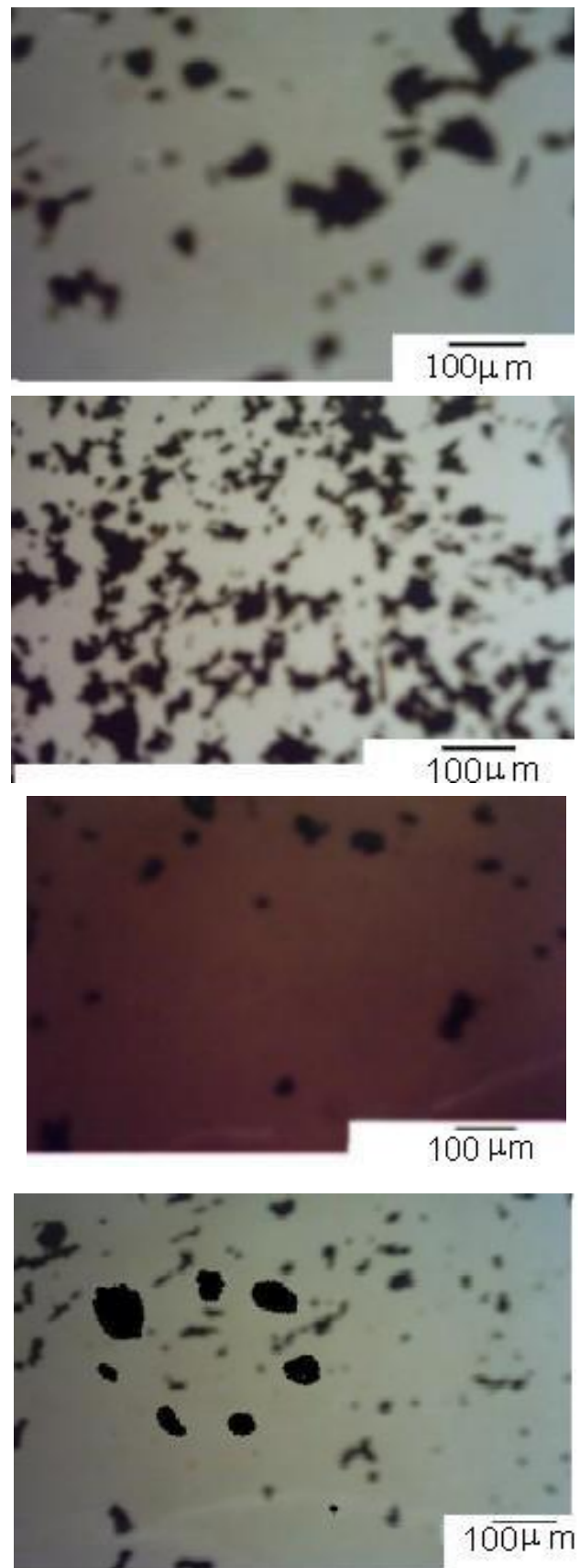


Figure 3: Microscopic photograph of Nickel powder suspended in oil at different particle sizes x100

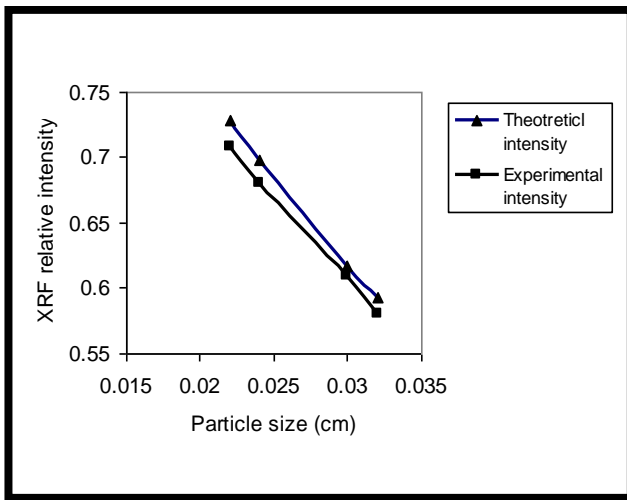


Figure 4: XRF relative intensity as a function of particle size for Fe powders suspended in Iraqi oil

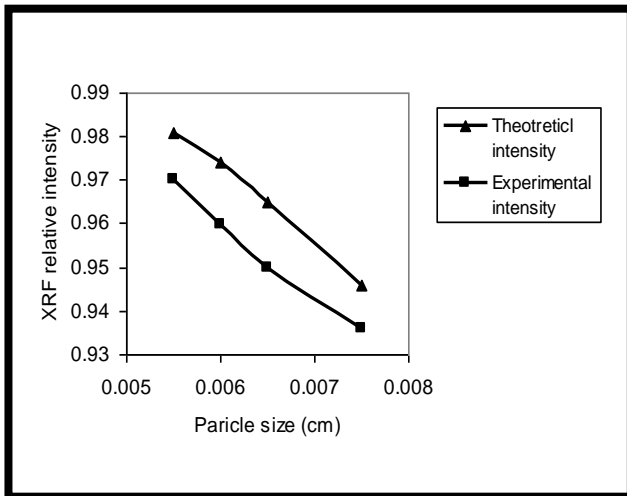


Figure 5: XRF relative intensity as a function of particle size for Co powders suspended in Iraqi oil.

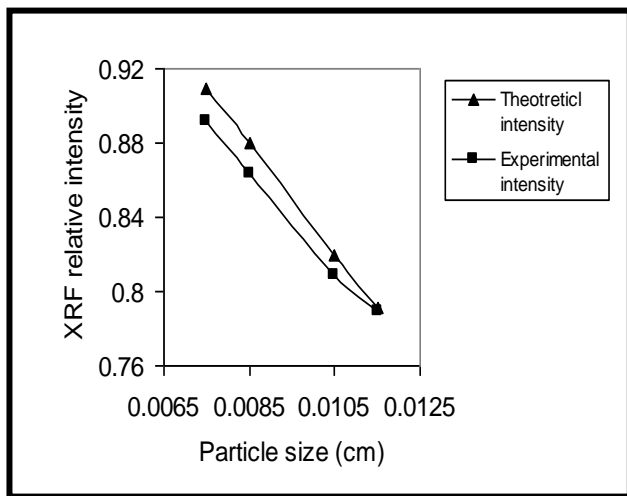


Figure 6: XRF relative intensity as a function of particle size for Ni powders suspended in Iraqi oil

4. Conclusions

From information gained in the present research certain conclusions may be draw regarding the X-ray fluorescent behavior of particles in oil suspension. Iron of 0.022 cm in size yielded about 71% the intensity of a real sample, an increase in fluorescence in size up to 0.032 cm results in a decrease in fluorescent intensity by at least 20%. Cobalt of 0.0055 cm in size yield about 97% the intensity of a real sample, an increase in fluorescence in size up to 0.0075 cm results in a decrease in fluorescent intensity by at least 5%. Nickel of 0.0075 cm in size yield about 90% the intensity of a real sample, an increase in fluorescence in size up to 0.0115 cm results in a decrease in fluorescent intensity by about 12%.

Good agreement between the theoretical and experimental relative intensity for samples was found.

References

- [1] Humphrey,G.R.; and Darrel, B.C.:(1998). the path to affordable long term failure warning, the XRF-monitor. International condition monitoring Conference, Alabama.
- [2] Abdulhadi Kadhium "Improvement the fatigue resistance and increase its life of specimens of naval brass alloy using laser shock wave processing" Journal of Nanoscience and Technology, 2(1) (2016) 69–726.
- [3] Tertian, R.; and Claisse,F. (1996). Principles of Quantitative X-ray fluorescence Analysis Hyden & sons Ltd.London.
- [4] Whitlock,R.R.:(1997). Filter debris analysis using XRF .proceeding of the 51st meeting of the society for machinery failure prevention technology (MFPT) .Virginia.
- [5] Jenkin, R.; (2000).X-ray technique. Encyclopedia of Analytical chemistry pp13269-13288 , John wiley & sons Ltd , chichester.
- [6] Jenkins, R. ; and Devries, J.L. (1970). Practical X-ray spectrometry Second edition , printed in Great Britain by Hazell Watson-Viney Ltd.
- [7] HaithamT.Hussein , Abdulhadi Kadhim , AhmedA.Al-Amiery , etal "Enhancement of the Wear Resistance and Microhardness of Aluminum Alloy by Nd:Yag Laser Treatment"The Scientific World Journal Volume 2014, Article ID 842062, 5 pages.
- [8] Abdulhadi Kadhim ,EvanT.Salim SaeedM.Fayadh AhmedA.Al-Amiery, AbdulAmirH.Kadhum, and AbuBakarMohamad3, "Effect of Multipath Laser Shock Processing on Microhardness, Surface Roughness, and Wear Resistance of 2024-T3 Al Alloy" The Scientific World Journal Volume 2014.
- [9] Havrilla, G.J., X-ray fluorescence spectrometry. Prentice Hall PTR , Newjersey 1997.
- [10] Gunn, E.L.; Advances in X-ray analysis. Vol.11, pp165-176. 1968.
- [11] A.H. Al-Hamdani1, M. Qasim1, K.S. Rida1, A. Kadhim2,* "Enhancement of Solar Cell Performance Based On Porous Silicon" Journal of Nanoscience and Technology 2(2) (2016) 73–75 .
- [12] Sutiana Junaedi , Abdul Amir H. Kadhum Ahmed A. Al Amiery, Abu Bakar Mohamad , Mohd Sobri Takriff " Synthesis and Characterization of Novel Corrosion Inhibitor Derived from Oleic Acid: 2- Amino-5-Oleyl-1,3,4-

- Thiadiazol (AOT)" *Int. J. Electrochem. Sci.*, 7(2012), 3543-3554.
- [13] Mark,B.; Berry, P.; and Voots, G.; (1995). Spectrace 9000 Field portable XRF . Congress on X-ray Analytical methods . pp1-6
- [14] Abdulhadi Kadhim ,Haitham T.Hussein “Enhancement of the Wear Resistance and Microhardness of Aluminum Alloy by Nd:YAG Laser Treatment” , *Scientific World Journal* , Volume 2014.
- [15] Emad Yousif, Ahmed A. Al-Amiery , Abdulhadi Kadhim, Abdul Amir H. Kadhum and Abu Bakar Mohamad”Photostabilizing Efficiency of PVC in the Presence of Schiff Bases as Photostabilizers”, *Molecules* 2015, 20, 19886–19899.
- [16] A Kadhim, Raid S Jawad, Najwan H Numan, Razi J Al-Azawi “Determination the wear rate by using XRF technique for Kovar alloy under lubricated condition” *International Journal of Computation and Applied Sciences IJOCAAS* Vol. 2, Issue 1, FEBRUARY 2017 .
- [17] Marketing specification of Iraqi petroleum production product.; (2000).
- [18] Hammad R. Humud†*, Abdulhadi Kadhim† and Lubna Abd Al Kareem “Gas Flow Rate Effect on the Nonlinear Optical Properties of Ag/Pmma Nanocomposite Thin Films Prepared by Aerosol Assisted Dielectric Barrier Discharge Plasma Jet Polymerization” *International Journal of Current Engineering and Technology*, Vol.5, No.5 2015.
- [19] A Kadhim, Hammad R Humud, Lubna Abd Al Kareem, “XRD and FTIR studies for Ag/PMMA Nano composite thin films” *International Journal of Computation and Applied Sciences IJOCAAS* Vol. 1, Issue 2, 2016 .